[Frontiers in Bioscience, 5, e36-52, June 1, 2000]

THE RENAL MEDULLARY MICROCIRCULATION

Aurélie Edwards [1], Erik P. Silldorff [2], and Thomas L. Pallone [3]

[1] Department of Chemical Engineering, Tufts University, [2] Department of Biology, Towson University, [3] Division of Nephrology, University of Maryland at Baltimore

TABLE OF CONTENTS

1. ABSTRACT

Blood flow to the renal medulla is supplied through descending vasa recta (DVR), which are derived from the efferent arterioles of juxtamedullary glomeruli. In addition to their role as conduits for blood flow, it is accepted that the vasa recta are countercurrent exchangers. That process, however, involves events which are more complicated than paracellular diffusive exchange of NaCl and urea. Urea transport in DVR is accommodated through the combined expression of endothelial and erythrocyte facilitated carriers while transport of water involves solute driven efflux across water channels. Unlike DVR, which have a continuous endothelium, ascending vasa recta (AVR) are fenestrated with a very high hydraulic conductivity. Transport of water in AVR is probably governed by transmural hydraulic and oncotic pressure gradients. The parallel arrangement of DVR in outer medullary vascular

bundles coupled with their capacity for vasomotion implies a role for regulation of the regional distribution of blood flow within the medulla The importance of the latter process in the urinary concentrating mechanism and the exchange of nutrients and O_2 is poorly defined. The large number of hormones and autacoids that influence DVR vasomotion, however, suggests that DVR have evolved to optimize the functions of the renal medulla.

2. INTRODUCTION

The microcirculation of the renal medulla plays a significant role in the urinary concentrating mechanism. In addition to delivering oxygen and other nutrients to tissue, vasa recta (i.e., the blood vessels in the renal medulla) must remove water added to the medullary interstitium by reabsorption from the descending limb of the loops of Henle and from the collecting tubules. Vasa recta must also preserve the corticomedullary concentration gradients of NaCl and urea that are generated and maintained by reabsorption of those solutes from nephrons. "Washout" of corticomedullary NaCl and urea gradients is prevented by the counter-current arrangement of descending (DVR) and ascending vasa recta (AVR). DVR and AVR have a number of surprising physiological and anatomical complexities. DVR are comprised of a continuous endothelium that expresses both water channels and a facilitated urea transporter. Pericytes (smooth muscle remnants) surround the DVR enabling them to contract and dilate in response to many hormonal stimuli. AVR have a fenestrated endothelium that imparts a remarkably high hydraulic conductivity. DVR and AVR are sequestered into vascular bundles in the outer medulla but become interspersed with nephrons in the inner medulla. Thus tubular-vascular relationships are complex and exhibit marked regional heterogeneity. These features demonstrate that the medullary microvasculature is complex and specialized to participate in the multiple physiological functions of the kidney.

3. VASA RECTA ANATOMY AND COUNTER-CURRENT EXCHANGE

3.1. Anatomy of the Renal Medulla

Nephrons in the kidney act as countercurrent multipliers that both dilute and concentrate the urinary filtrate. In the vasopressin stimulated, concentrating kidney, the tubular fluid and interstitial osmolality increases steadily from the corticomedullary junction to the papillary tip, reaching values which exceed plasma osmolality by factor of 3 to 10 depending on the species. The renal medulla is divided into an outer and an inner region; the outer medulla is further subdivided between an outer and an inner stripe. Blood vessels in the outer medulla are grouped into vascular bundles which are separated from the nephron segments which lie in the interbundle region. In the inner medulla, the vessels are more evenly dispersed between the collecting ducts and thin limbs of Henle's loops.

The renal artery branches into interlobar arteries that ascend within the renal pelvis, enter the renal parenchyma, change course and become arcuate arteries as they run near the corticomedullary border. Arcuate arteries give rise to interlobular arteries (cortical radial arteries), which ascend through cortex toward surface of kidney, and from these afferent arterioles originate. The efferent arterioles of juxtamedullary glomeruli cross the cortico-medullary junction to enter the outer stripe of the outer medulla where they give rise to descending vasa recta (DVR). Among the DVR running through the outer medulla, those that supply the inner medulla pass through the center region of the vascular bundles, where they communicate with ascending vasa recta (AVR) returning from the inner medulla. Those DVR that supply the capillary plexus of the outer medulla, where nephrons reside, lie on the periphery of the bundles and peel off to form the dense capillary plexus of the interbundle region. The AVR arising from the capillary plexus in the outer medullary interbundle region do not lie within vascular bundles. They return directly to the cortex without rejoining the vascular bundles.

The structural properties of DVR and AVR differ considerably. The DVR have continuous endothelial cells and intercellular tight junctions, whereas the AVR have a highly fenestrated endothelium, suggesting a higher permeability to water and small solutes. In the inner medulla, DVR give rise to many AVR. AVR are also larger than DVR (20 microns vs. 15.6 microns, respectively) (1). These features result in a slower velocity of blood flow and exposure to a larger vessel wall surface area on the ascending (venous) side of the circuit.

3.2. Vasoconstriction of Descending Vasa Recta

Juxtamedullary efferent arterioles are surrounded by a layer of smooth muscle cells. In DVR, these cells are replaced by pericytes, which impart contractile properties to these vessels (Figure 1). Outer medullary DVR (OMDVR) constrict in response to angiotensin II (2), endothelin (3), norepinephrine (4), and vasopressin (5). Vasoconstriction of OMDVR can be abrogated by hormones produced locally within the medulla such as prostaglandin E_2 (2,3) and adenosine (6).

Since the majority or all blood flow to the renal medulla travels through OMDVR, these vessels probably play a fundamental role in the regional regulation of blood flow to the medulla. It seems conceivable that dilation of vessels on the bundle periphery (or constriction of those in the bundle center) would favor enhancement of perfusion of the outer medullary interbundle region where oxygen and energy requirements may be high for the avidly NaCl reabsorbing thick ascending limb. Several vasoactive hormones, such as prostaglandins, adenosine, kinins and endothelins, are synthesized within the inner medulla. If they are trapped by the microcirculation, as AVR blood flows back from the inner medulla to the cortex through the vascular bundles, it seems likely that they could act on DVR in the bundles, giving rise to possible feedback regulation of inner medullary blood flow.

3.3. Counter-Current Exchange: General Principles

The function of a counter-current exchanger is to maximize transfer between its limbs and their surroundings so as to minimize the net removal of solute or heat from the

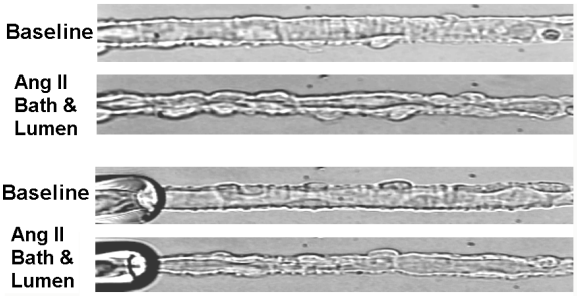

Figure 1. Vasoconstriction of descending vasa recta. Examples of outer medullary DVR from vascular bundles of rats. The vessels have been isolated by microdissection, transferred to an inverted microscope, cannulated with pipettes and perfused. Two vessels are shown in both the baseline state and after vasoconstriction through application of angiotensin II at 10^{-8} M to the bath and lumen. Two cell types can be seen in the wall of the vessels. The cell bodies of the smooth muscle remnants, known as pericytes protrude from the abluminal surface. Endothelial cells line the lumen of the vessels.

surrounding medium. The exchanger removes solute or heat from its environment by diffusive influx during inflow and returns it to the environment by efflux during outflow. In the renal medulla, the counter-current arrangement of DVR and AVR is necessary to preserve cortico-medullary gradients, which would otherwise be dissipated by blood flow. In a perfectly efficient exchanger there would be no net loss from the surroundings. The latter is theoretically achieved when the limbs of the exchanger achieve infinite permeability or flow through the exchanger approaches zero. Of course, the permeability of the limbs is always finite and flow is nonzero so that real exchangers always carry away some solute or heat from the regions they perfuse.

The factors that govern the efficiency of a counter-current exchanger can be examined using a simplified model. Assuming volume flow rate through the lumen (Q) is constant, and that the descending and ascending limbs have the same permeability (P), the transmembrane solute flux (J_s) from lumen to interstitium is given by:

Equation 1

$$J_S = P(C - C_i)$$

where C and C_i are the solute concentration in the limb and in the interstitium, respectively. If the interstitium is less concentrated than the limb, the solute will diffuse out of the lumen, and vice-versa. If the solute concentration rises linearly in the interstitium,

Equation 2

$$C_i = C_{io} + \Delta C \frac{x}{L}$$

where C_{io} and ΔC are given constants, x denotes the axial coordinate, and L is the total length of the counter-current exchanger.

It can be shown that the luminal concentrations on the descending (C_d) and ascending (C_a) sides are given by (7),

Equations 3a, 3b

$$C_d = C_{io} + \Delta C \frac{x}{L} + \frac{\Delta C}{l}\{\exp(-\frac{lx}{L}) - 1\}$$

$$C_d = C_{io} + \Delta C \frac{x}{L} + \frac{\Delta C}{l}\{\exp(-l(2-\frac{x}{L})) - 2\exp(-l(1-\frac{x}{L})) + 1\}$$

Since the first two terms on the right hand side of equations (3a, 3b) correspond to the interstitial concentration, the third one represents the concentration difference across the vessel wall. Concentration profiles are plotted in Figure 2 for different values of λ. As the luminal fluid flows through the descending limb, diffusive solute influx occurs so that concentration increases. The derivative of the third term is negative in equation 3a, reflecting the fact that solute concentration in the descending limb increasingly lags behind that in the interstitium as the fluid flows into a region of increasing osmolality. After the hairpin turn, solute concentration in the ascending limb keeps increasing until it becomes equal to that in the interstitium. It then starts to fall, but not as fast as the interstitial concentration does, and solute diffuses out of the lumen. The solute is thus trapped and recycled as it diffuses from the interstitium into the descending limb and out of the ascending limb back to the interstitium.

As indicated by *equations 3a and 3b*, the two parameters governing the magnitude of these variations are ΔC and λ. The larger the axial gradient in the interstitium (i.e., ΔC), the larger the transmural concentration differences between the limbs and the interstitium. Indeed, when axial gradients are steep, transmural gradients must also increase to give rise to the large solute fluxes that are needed to concentrate and then dilute the luminal fluid. A higher flow rate (i.e., a lower λ) also increases transmembrane differences, as shown in Figure 2, since the luminal fluid then requires higher influx rates to concentrate. In contrast, a high permeability (i.e., a higher λ) results in a smaller lag between luminal and interstitial concentration, as the magnitude of transmural fluxes is then increased.

The efficiency of the counter-current exchanger is inversely related to the rate at which solute is removed from the interstitium, that is, the difference between the mass flow rate of solute leaving and entering at x = 0. For the above simple model, this is given by:

Equation 4

$$\Delta M = Q(C_{ao} - C_{do}) = \Delta C \frac{Q^2}{PS}\{\exp(-2l) - 2\exp(-l) + 1\}$$

where the subscript "o" indicates that the concentrations are evaluated at x = 0. Since the rate of removal increases with the square of the flow rate, a higher Q decreases efficiency. Conversely, the higher the permeability or the limb surface area, the smaller ΔM and the more efficient the exchanger.

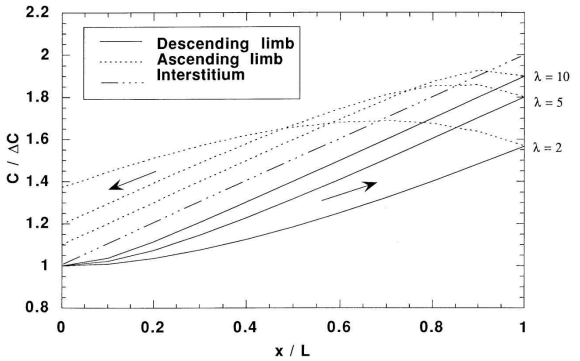

Figure 2. Solute concentrations in an idealized countercurrent exchanger. Ratio of solute concentration (C) in limbs of exchanger and in interstitium to total increase in solute concentration along axis of exchanger (? C), as a function of normalized distance along the exchanger (x/L) and for different values of λ = PS/Q. Arrows indicate direction of flow in limbs of exchanger.

Thus, very permeable walls and a large area of contact between the limbs and the interstitium are required to maximize radial exchanges and thus efficiency.

Counter-current exchange in the renal medulla is far more complicated than the process described above. The numbers of vasa recta vary along the cortico-medullary axis, there are more AVR than DVR at any given point along the axis, and DVR and AVR have different diameters. In addition, transmural volume fluxes are not zero but depend significantly on small solute concentration gradients, as well as hydraulic and oncotic pressure differences. In spite of these and other differences, the main conclusions drawn from the simple exchanger presented above will remain valid; optimum efficiency is obtained with high permeabilities and low flow rates. In the two sections that follow, blood flow rate and permeability measurements are discussed.

4. BLOOD FLOW IN VASA RECTA

4.1. Techniques and Measurements

Regional blood flow within the kidney has been intensively investigated by a variety of techniques. Early methods focused on monitoring tracer movement through the kidney. More recently, laser-Doppler and video-microscopy have allowed for direct examination of regional perfusion. Many reviews on this topic have appeared (7-10).

4.1.1. Cortical Extraction of PAH

This method was based upon the assumption that p-aminohippurate (PAH) is completely extracted from plasma in the renal cortex but not in the medulla, so that the difference between unity and the extraction ration times the renal plasma flow should be equal to the medullary blood flow. However, extraction of PAH from renal arteriole blood is not complete but varies with blood flow rate and hematocrit (11) and secretion of PAH occurs in the pars recta of the outer medulla (12). This method has thus been largely discounted.

4.1.2. Diffusible Tracers

Highly diffusible tracers, such as inert gases, circulate to the kidney after systemic injection and become distributed within the parenchyma. The organ concentration of tracer then decays exponentially with time. Since blood flows to several compartments in the kidney, the overall tracer content is given by the sum of exponential terms, each of which corresponds to one compartment and depends upon its blood flow, partition coefficient, and volume. By injecting ^{85}Kr into the renal artery of dogs, Thornburn *et al.* (13) identified four components to the decay curve, corresponding to disappearance from the outer cortex, the inner cortex and the outer medulla, the inner medulla, and the perirenal and hilar fat, respectively. Estimates of blood flow to the outer and inner medulla (1.32 and 0.17 ml min^{-1} g^{-1}, respectively) were thought to be underestimated due to counter-current trapping of ^{85}Kr. Aukland and co-workers (14-16) administered hydrogen as a tracer to anesthetized dogs by inhalation or injection. Oxidation of H_2 at platinum electrodes produces a current proportional to its local concentration. Hydrogen disappearance from specific regions of the kidney was thus monitored through inserted platinum electrodes, and cortical blood flow was estimated as 2.6 to 5.0 ml min^{-1} g^{-1}. Because of hydrogen recirculation in the medulla, no reliable estimate of medullary blood flow rate was obtained. More recently, Parekh and colleagues (17) have shown that hydrogen can be locally generated and simultaneously detected using implanted platinum electrodes, so that changes in the local H_2 concentration reflect variations in local blood flow rates, thereby providing a way to measure regional perfusion. Attempts to use heat as a diffusible tracer have been hampered by the fact that the amount of heat lost by conduction is not negligible relative to convective dissipation arising from local tissue perfusion. Heat conduction towards the kidney surface is too rapid to allow for separate measurements of convective losses, and local tissue thermodilution is not a reliable measure of tissue blood flow.

4.1.3. Rubidium Extraction

The amount of a radio-labeled indicator flowing to a given organ is proportional to the fraction of cardiac output that the organ receives. If the indicator is completely extracted, so that no recirculation occurs, or if the organ extraction ratio remains constant and equal to the systemic extraction ratio, the amount of tracer recovered from the organ can be related to the local blood flow. This technique was first used by Sapirstein (18), with the isotopes ^{42}K and ^{86}Rb. The rubidium uptake method has been critically examined by several investigators and most recently upheld by Karlberg *et al.* (19), who reported blood flows to the cortex, outer stripe, inner stripe, and inner medulla equal to 5.2, 2.2, 1.5, and 0.69 ml min^{-1} g^{-1}, respectively.

4.1.4. Indicator Transit Time

If an indicator restricted to the intravascular space is injected into the renal artery, its mean transit time at a given point in the vascular bed is equal to the ratio of the volume in which the indicator is dispersed to the regional blood flow. Mean transit time is generally estimated by

dividing the area under the concentration-time curve by the peak concentration. Transit time indicators have included tracers bound to albumin (e.g., Evans blue dye and ^{131}I) or red blood cells, together with photoelectric sensors or beta-sensitive semiconductors.

4.1.5. Albumin Accumulation

After injection of radiolabeled albumin, total accumulation in the inner medulla provides a measure of medullary blood flow, provided that there is no rapid washout of albumin from the medulla. The albumin accumulation technique was developed by Lilienfield and coworkers (20-22) who injected ^{131}I albumin into the ascending aorta of dogs, tied off the renal pedicle at timed intervals, and quickly froze the kidneys. The authors observed a linear increase in the volume of distribution of albumin up to one minute after injection and determined a papillary plasma flow rate of 0.25 ml min^{-1} g^{-1}. To eliminate time changes in plasma tracer concentration, Rasmussen (23,24) devised a method involving the cross-circulation of an experimental rat and a "pump" rat. His estimates of medullary blood inflow rates were between 0.38-0.64 and 0.060-0.084 ml min^{-1} g^{-1} for plasma and RBCs, respectively.

4.1.6. Microspheres

As noted by Sapirstein (18), the ideal tracer for blood flow measurements would undergo complete extraction, so that the amount of tracer recovered from the organ would be proportional to the blood flow to that organ. McNay and Abe (25) used radiolabeled microspheres for that purpose, and reported that microspheres greater than 10 ? m in diameter were completely trapped within the preglomerular or glomerular circulation, whereas 3-30% of microspheres less than 7 microns in diameter reached the venal rein. Use of microspheres to measure regional blood flow to the cortex has shown that reductions in renal perfusion pressure, or hemorrhage, results in a redistribution of blood flow to favor perfusion of juxtamedullary glomeruli. By injecting microspheres of 15±5 microns in rabbits and subsequently dissecting glomeruli from various cortical regions, Bankir *et al.* (26) determined that 9% of the renal blood flow reaches the medulla. Because of size dispersion in microspheres, several investigators have examined whether this method overestimates and underestimates blood flow to superficial and juxtamedullary glomeruli, respectively. Larger microspheres tend to accumulate near the axis of interlobular arteries, thus preferentially reaching superficial glomeruli; because the radioactivity present in a microsphere is proportional to its radius to the third power, these streaming effects might result in overestimation of superficial cortical flow. The conclusions from various such studies have differed widely, and the use of microspheres to determine regional blood flow within the cortex remains questionable.

4.1.7. Laser-Doppler

When a monochromatic light from a helium-neon laser is focused on a small area of tissue, the frequency of light scattered by RBCs undergoes a Doppler shift. The signal from the reflected light is proportional to RBC velocity and number. Roman and Smits (27) used this technique to measure papillary blood flow in young Munich-Wistar and adult Sprague-Dawley rats. They obtained a linear correlation (R=0.92) between the laser-Doppler blood flow signal from the papilla and RBC inflow rates as determined by the accumulation of ^{51}Cr-labeled RBCs. Papillary blood flow was found to be 0.18 and 0.31 ml min^{-1} g^{-1} in young and older rats, respectively. In theory, the laser-Doppler has to receive random back-scattered light, and the organized counter-flow arrangement of vasa recta would appear to violate that requirement. Yet, agreement between results based on this method and other techniques (27,28) has alleviated that concern. The laser-Doppler method offers many advantages, among which the ability to perform multiple measurements in the same region. Measurements can also be obtained on the renal surface or with flow probes implanted at various depths into the renal parenchyma.

4.1.8. Videomicroscopy

Measurements of RBC velocity, combined with knowledge of micro-vessel diameter, can yield estimates of capillary blood flow rate. This approach was initially adapted to studying regional blood flow in the kidney by Marsh and Segel (29), with subsequent refinements using videomicroscopy. Gussis *et al.* (30) measured RBC velocity in individual vasa recta on the surface of the exposed renal papilla. Holliger and colleagues combined measurements of RBC velocity and capillary diameter to determine single vasa recta blood flow rate (1). In more recent developments, the papilla was illuminated by fluorescent light and viewed through a highly sensitive silicon intensified target camera. Contrast between red cells, plasma and the capillary wall was enhanced by injection of fluorescein isothiocyanate gamma globulin. The dual-slit technique was adapted to videomicroscopy, and the time delay between upstream and downstream signals, which is equal to the transit time for RBC's between the two windows, was derived by computer cross correlation. Blood velocity differs from that of RBC's due to the Fahreaus effect. The relationship between the two was determined using quartz capillaries (31,32). While this method has provided important data, it is limited in the medulla by the accessibility of the microcirculation. Videomicroscopy of the medulla is only possible in the papilla, which must be exposed by surgical immobilization of the kidney and excision of the ureter, an experimental maneuver that may increase medullary blood flow (33).

4.1.9. Micro-vessel diameter measurements

In addition to methods that measure tissue or single vessel blood flow rates, it is also possible to assess the effects of vasoactive hormones by measuring the diameter changes that occur in pressurized micro-vessels. This is done on micro-vessel segments that have been dissected and perfused *in vitro* on glass pipettes or on vessels observed *in situ* within tissue preparations. These approaches provide important information on the sites of action and concentrations at which vasoactive substances modulate vasomotor tone. The methods are, however, subject to artifacts. Damage may result from preparation and the local interactions of vessels with the interstitium

and extracellular matrix are altered. Several reviews have described these approaches and their limitations (7-12).

4.2 Intrarenal Hematocrit

Indirect (radiolabeling) and direct (videomicroscopy, micropuncture) measurements of the volumes of distribution of plasma and RBC's within the kidney have consistently shown that medullary hematocrit is significantly lower than systemic hematocrit. Most recently, using videomicroscopy, Zimmerhackl *et al.* (31) determined the capillary hematocrit to be 26 and 25 % in DVR and AVR, respectively, in animals whose mean hematocrit was 44 %. Several explanations have been invoked. Given that RBC's travel preferentially near the vessel center (see below), Pappenheimer and Kinter (34) proposed that the relatively cell-free blood near the walls is "skimmed" from the periphery of he interlobular arteries to enter the afferent arterioles of deep glomeruli. By that mechanism, superficial glomeruli would receive blood of high hematocrit whereas juxtamedullary glomeruli would receive blood of low hematocrit. The plasma skimming theory has been extensively investigated, but no agreement has been reached. Lilienfield *et al.* (21) measured the distribution of radiolabeled albumin and RBC's in different regions of the kidney and failed to detect the gradient of tissue hematocrit from inner to outer cortex predicted by the plasma skimming theory. However, they did find such a gradient in the medulla, where RBCs occupy 10.4 ml/100 g of tissue in the outer medulla but only 3.5 ml/100 g of tissue at the papillary tip. Rasmussen (23) injected simultaneously ^{51}Cr-RBCs and ^{131}I immunoglobulin M (IgM), a larger and therefore more reliable plasma marker than albumin, and determined that the ratio of tissue hematocrit to systemic hematocrit was 0.85-0.95 for the whole kidney, cortex, and outer medulla, and 0.45-0.60 in the inner medulla. Consistent with the hypothesis of Pappenheimer and Kinter (34), he found that the ratio of RBC-to-albumin inflow rate was reduced in the renal medulla, implying separation of RBC and plasma flows somewhere between the renal artery and the medullary microcirculation (24). The importance of plasma skimming to urinary concentration remains uncertain, and the other mechanisms described below may be sufficient to account for low vasa recta hematocrit.

Since vasa recta diameter are 10-20 microns, the Fahreaus effect is expected to be of importance. Fahreaus (35) demonstrated that micro-vessel hematocrit (i.e., the ratio of RBC volume to total capillary volume) is less than that of the large vessel what supplied it. Indeed, RBCs migrate to the center of the axial blood stream in small vessels, and they travel at higher velocities than the cell-free plasma near the vessel walls, which is retarded by friction. Consequently, blood of low hematocrit flows slowly in the periphery of the stream, and the intra-capillary tube hematocrit (H_T) is lower than the discharge hematocrit (H_D), i.e., the hematocrit that would be obtained if blood flowing in the capillary was collected and spun in a centrifuge. In general, H_D is equal to the hematocrit of the large feeding vessel. In vessels with diameters similar to those of vasa recta, the ratio of H_T to H_D should be between 0.5 and 0.6 (36).

Moreover, a "network" Fahreaus effect may also lower hematocrit in the vasa recta. Pries *et al.* (37) showed that as much as 20% of the hematocrit reduction in the capillary bed of the rat mesentery could be due to this network effect. At micro-vessel bifurcations, the branch with the higher flow rate receives blood of higher hematocrit. Conservation of RBC and plasma volume requires that the increase in hematocrit in high-flow branches be less than the decrease in low-flow branches, thereby further reducing the average capillary hematocrit. Finally, shrinkage of RBC's in the hypertonic medulla shifts volume from erythrocytes to plasma (7) and thus also contributes to lower medullary micro-vessel hematocrit.

5. PERMEABILITY OF VASA RECTA

5.1. To Water

The permeability of vasa recta to water has been determined using different techniques, with similar results. Pallone and co-workers microperfused Munich-Wistar rat vasa recta with a solution containing impermeant fluorescent dextran and 0.1 g/dl albumin (a small concentration prevents the alteration of micro-vessel hydraulic conductivity that would result in the complete absence of albumin). The rate of volume efflux was related to the perfusion rate and the perfusate-to-collectate concentration ratio. The hydraulic conductivity of DVR was thus estimated to be between 1.4 and 3.4 $x10^{-6}$ cm s^{-1} $mmHg^{-1}$ (38), that of AVR between 12.5 and 18.7 $x10^{-6}$ cm s^{-1} $mmHg^{-1}$ (39). The larger permeability of AVR is predicted by their highly fenestrated endothelium (40). The hydraulic permeability of AVR was also measured by MacPhee and Michel (41), using a modification of the micro-occlusion technique in which Sprague-Dawley rat AVR were perfused with a suspension of red cells filled with Evans Blue. Their estimates ranged between 30 and 200 $x10^{-7}$ cm s^{-1} cmH_2O^{-1}, with a mean value of 92 $x10^{-7}$ cm s^{-1} cmH_2O^{-1}, that is, 12.5 $x10^{-6}$ cm s^{-1} $mmHg^{-1}$, in very good agreement with the results of Pallone (39).

Measurements of the osmotic water permeability (P_f) of DVR, corresponding to the transcellular pathway through water channels, were obtained by Pallone *et al.* (42). To eliminate the contribution of the paracellular pathway, water transport was induced with transmural NaCl gradients, yielding P_f = 1085 microns s^{-1}. A summary of these values is provided in Table 1.

5.2. To Sodium and Urea

The permeability of vasa recta to small solutes was first measured by Morgan and Berliner (43), and Marsh and Segel (29). The most recent estimates of permeability to sodium (P_{Na}) and urea (P_u), reported by Pallone and coworkers (44), were obtained by microperfusing inner medullary vessels *in vivo* and outer medullary DVR *in vitro* and measuring the lumen-to-bath efflux of ^{22}Na and ^{14}C-urea. In the inner medulla, P_{Na} and P_u were always nearly identical and highly correlated suggesting simultaneous diffusion without steric restriction through an aqueous pore. The permeability of papillary AVR to sodium and urea was determined as 115 and 120

Table 1. Hydraulic conductivity (Lp), osmotic water permeability (P_f) and reflection coefficients

Parameter	Driving Force	OMDVR	IMDVR	IMAVR	Reference
L_p x 10^{-6} ($cm \bullet s^{-1} \bullet mmHg^{-1}$)	Albumin Gradient		1.4 [A]		38
L_p x 10^{-6} ($cm \bullet s^{-1} \bullet mmHg^{-1}$)	Albumin Gradient	1.6			49
L_p x 10^{-6} ($cm \bullet s^{-1} \bullet mmHg^{-1}$)	NaCl Gradient	0.12 [B]			42
L_p x 10^{-6} ($cm \bullet s^{-1} \bullet mmHg^{-1}$)	Hydraulic Pressure			12.5	39,41
Parameter	**Method**	**OMDVR**	**IMDVR**	**IMAVR**	**Reference**
$\sigma_{albumin}$	Sieving	0.89 [C]			49
$\sigma_{albumin}$	Sieving			0.78	48
$\sigma_{albumin}$	Osmotic			0.70	41
σ_{Na}	Osmotic	~ 0.03 [D]			55
σ_{Na}	Sieving	~1.0 [E]			55
$\sigma_{Raffinose}$	Sieving	~1.0 [E]			55

[A] Assumes a reflection coefficient to albumin of 1.0., [B] Evidence shows that transmural NaCl gradients drive water flux exclusively through water channels, whereas albumin drives water flux predominantly through water channels along with a small component via other pathway(s)., [C] Not significantly different from 1.0., [D] Measurement of σ_{Na} for the vessel wall as a whole., [E] σ_{Na}, $\sigma_{Raffinose}$ for the aquaporin-1 water channel pathway through which NaCl gradients drive water flux.

$x10^{-5}$ cm s^{-1}, respectively; that of papillary DVR to sodium and urea was measured as 75 and 76 $x10^{-5}$ cm s^{-1}, respectively. Outer medullary DVR, however, were four times more permeable to urea (360 $x10^{-5}$ cm s^{-1}) than to sodium (75 $x10^{-5}$ cm s^{-1}). These results, together with the observation that transport of ^{14}C-urea was reversibly inhibited by addition of unlabeled urea analogues or phloretin to the bath and lumen, showed the existence of a transcellular pathway for urea in OMDVR, through which transport is carrier-mediated. Although the findings of Pallone *et al.* (44,45) suggested the absence of the transporter in the inner medulla, recent *in situ* hybridization experiments have shown that the urea-transporter isoform UT3 is expressed in outer medullary DVR as well as in papillary DVR (46). The transporter UT3 is the rat homologue of the erythrocyte urea transporter, also found in human outer and inner medulla DVR (47). The disparity between urea transport properties measured by microperfusion of inner vs outer medullary DVR may be explained if tracer efflux during microperfusion *in vivo* is limited by the buildup of ^{14}Curea in the papillary interstitium, outside the vessel wall. *In vitro* perfusion of DVR, which can only be performed on outer medullary vessels, is far less subject to effects of unstirred layers because a flowing buffer bathes the abluminal surface. A summary of permeability properties is provided in Table 2.

5.3. To Albumin

Due to experimental limitations, the very low permeability of vasa recta walls to albumin has not yet been reliably determined. An important determinant of trans-capillary volume fluxes, the reflection coefficient of AVR walls to albumin (σ_a), was recently measured by several investigators. Based upon the changes in the effective oncotic pressure exerted by perfusates containing different concentrations of bovine serum albumin (BSA), MacPhee and Michel (41) obtained estimates of σ_a between 0.59 and 0.72. Pallone (48) compared the ultrafiltration of ^{125}I-albumin by AVR with that of FITC-dextran and reported a value of 0.78. A similar technique was used by Turner and Pallone (49) to determine the reflection coefficient of OMDVR walls to albumin, yielding an estimate of 0.89 (not significantly different from 1.0).

Several studies have shown that albumin is present in the medullary interstitium in significant concentrations (50,51). The mechanisms by which this extravascular pool of albumin is generated and maintained remain to be completely elucidated. Pallone (51) suggested that DVR are the source of interstitial proteins, and that the accumulation of albumin in the interstitium is governed by convective rather than diffusive processes. Since water reabsorption into AVR is driven by oncotic pressure differences, proteins must be continually removed from the interstitium; otherwise, increasing interstitial protein concentrations would abolish the very driving force responsible for fluid uptake, as discussed by Michel (52) and Levick (53). Radiolabeled albumin injected in the medullary interstitium is rapidly removed (41), but it is unclear how. Lymphatics are absent in the inner medulla and sparse in the outer medulla, and the possibility of clearance of albumin by drainage via pre-lymphatic channels is not supported by experimental evidence (41).

The most likely mechanism is that of protein clearance by the microcirculation itself. In the medulla, fluid absorption (into AVR) need not be a self-canceling process, because of the existence of a continuous influx of protein-free fluid into the interstitium from the loops of Henle and the collecting duct, which tends to dilute interstitial proteins. Since the reflection coefficient of DVR walls to albumin appears to be greater than that of AVR walls, it is possible in principle to maintain steady fluxes of albumin from DVR through the interstitium to AVR (41). Experimentation and mathematical simulations are needed to confirm whether albumin is indeed carried into and cleared from the interstitium by convective trans-capillary fluxes, or whether an active mechanism such as transcytosis could also play a role.

6. FACILITATED TRANSPORT PATHWAYS

6.1 Aquaporin-1 Water Channels

Aquaporin-1 water channels (AQP1) have been immuno-localized to DVR (54) and OMDVR contain sufficient AQP1 to account for osmotic water permeability

Table 2. Permeability of vasa recta to hydrophilic solutes

Permeability x 10^{-5} cm/s	**Species**	**OMDVR[A]**	**IMDVR[B]**	**IMAVR[B]**	**Reference**
P_{Na}	Hamster		28	51	29
P_{Na}	Rat	76	75	115	44
P_{Urea}	Rat		47		43
P_{Urea}	Rat	360	76	121	44
P_{Urea}	Rat	343 -> 191 [C]			45
P_D	Rat	476 [D]			54
$P_{raffinose}$	Rat	40			49,146
Permeability Ratio	**Species**	**OMDVR[A]**	**IMDVR[B]**	**IMAVR[B]**	**Reference**
P_{Urea} / P_{Na}	Rat		1.09	0.98	146
P_{Cl} / P_{Na}	Rat	1.33			
$P_{raffinose}$ / P_{Na}	Rat	0.35			
P_{Inulin} / P_{Na}	Rat	0.22			

Abbreviations: OMDVR, outer medullary descending vasa recta; IMDVR, inner medullary descending vasa recta; IMAVR, inner medullary ascending vasa recta., [A] Values obtained with *in vitro* microperfusion are highly dependent upon perfusion rate., [B] Values obtained with *in vivo* microperfusion in the exposed papilla are probably underestimated due to boundary layer effects., [C] Values are before and after inhibition with 50 mM thiourea., [D] P_D is diffusional water permeability measured by ^3H_2O efflux.

measured with transmural gradients of NaCl (42). In addition, volume efflux from OMDVR driven by transmural osmotic pressure gradients of NaCl occurs through a pathway that excludes 22Na and 3Hraffinose (55), providing evidence for a "water only" pathway across the DVR wall. The ability of p-chloromercuribenzenesulfonate (pCMBS), a known inhibitor of the AQP1 water channel, to entirely suppress water transport driven by NaCl gradients favors the interpretation that small solute induced water flux is mediated by water channels and that other transmural pathways must have a negligible reflection coefficient to NaCl. The existence of a parallel or "shared" pathway in OMDVR, across which water transport is driven by classical Starling forces, was recently confirmed (49). Small hydrophilic tracers diffuse across the latter pathway without steric restriction (54). These observations contradict the assumptions of previous models of the medullary microcirculation, which simulated the experimentally observed volume efflux from DVR by assuming only the existence of a "shared" pathway with a small non-zero reflection coefficient to sodium and urea. The specific role of AQP1 and urea-transporters in the medullary microcirculation must be re-evaluated.

6.2. Urea Transporter

In addition to AQP1, DVR endothelia express a facilitated urea carrier (44,45). This transporter is identical to that expressed by the red blood cell membrane and distinct from that expressed by the collecting duct and thin limbs of Henle (46,47). AVR blood returning from the renal inner medulla contains high concentrations of urea. That urea leaves the AVR lumen by diffusing down its concentration gradient into the interstitium from which it can then diffuse into the DVR lumen across DVR endothelial cells via a urea carrier. It is interesting to note that the same facilitated carrier is expressed by DVR endothelia and by the RBC to optimize equilibration between its interior and vasa recta plasma.

7. Models of Microcirculatory Function

Models of the urinary concentrating mechanism have generally neglected the role of vasa recta by assuming that the capillaries offer negligible resistance to transport of solute and water and lumping the DVR, AVR and interstitium into a "central core" (56,57). Such models, which focus on the counter-current multiplier function of the loop of Henle, proceed on the assumption that any finite inefficiency of countercurrent exchange will result in reduction of the model's prediction of maximal concentrating ability. The central core approach is a reasonable point of departure but must fail to capture the true relationship between microcirculatory function and the concentrating mechanism. Ultrastructural heterogeneity between DVR and AVR, the existence of facilitated pathways in DVR, and anatomical differences of tubular vascular relationships between the outer and inner medulla all suggest that the microvasculature plays a significant role to regulate the trafficking of sodium and urea. A satisfactory model of the concentrating mechanism that incorporates the loop of Henle and the medullary microcirculation with trans-capillary driving forces and endothelial resistance to transport would be very complex and has yet to be developed.

7.1. Early Models

The first model of the medullary microcirculation was that of Thurau *et al.* (58). A single vascular loop was considered, idealized as a U-shaped tube with limbs separated by a delimiting membrane. Transmural volume flow was entirely neglected, and solute flux into the tube was assumed to be constant. The model predicted that plasma solute concentration rises towards the papillary tip, and that concentrations are higher in AVR than in DVR at any given point along the cortico-medullary axis. Palatt and Saidel (59) later incorporated time-dependent responses in a similar approach.

Marsh and Segel (29) then developed a more detailed model in which the differences in number, diameter, and solute permeability between DVR and AVR observed in the golden hamster were accounted for. Solute transport across AVR and DVR was governed by diffusion only. Assuming that the DVR, AVR and the interstitium only exchange fluid and solutes with one another, solute

concentrations in all three compartments were determined. Marsh and Segel (29), however, assumed that vasa recta were located within vascular bundles throughout their length, so that their approach would only be valid for some vessels in the outer medulla. The other main limitations to their model were that it did not include transmembrane volume exchange nor transport between vasa recta plasma and RBC's.

7.2. Recent Models

Measurements of trans-capillary driving forces by Sanjana and colleagues (1975) stimulated new modeling efforts. Pallone *et al.* (60) considered one vascular unit with a single DVR extending from the cortico-medullary junction to the papillary tip, and giving rise to AVR in numbers consistent with ratios of AVR and DVR measured in rats and hamsters. Transmural water fluxes were related to protein and small solute concentrations in the vasa recta and interstitium by (61):

Equation 5

$$J_V^P = L_P[\Delta P - s_P \Delta p - RT \sum_S s_S g_S (C_S - C_S^I)]$$

where J_v^P is the plasma volume flux (positive if efflux occurs), L_p is the hydraulic conductivity, ΔP is the trans-capillary hydraulic pressure difference, $\Delta\pi$ is the trans-capillary oncotic pressure difference, R is the gas constant and T the temperature. C_s and C_s^I denote the concentrations of solute s in plasma and intersititium, respectively, σ_p and σ_s are the reflection coefficients of the capillary membrane to proteins and solute s, respectively and γ_s is the activity coefficient of solute s. The existence of water channels in DVR was unknown and σ_s was assumed to be a small but non-zero number (see below). Pallone *et al.* (60) also accounted for both diffusion and convection in determining trans-capillary solute fluxes:

Equation 6

$$J_S = J_V(1 - s_S)\frac{1}{2}(C_S + C_S^I) + P_S(C_S - C_S^I)$$

where J_s is the transmembrane flux of solute s and P_s is the vessel permeability to that solute. Interstitial concentrations of NaCl and urea were specified as inputs to the model. Red blood cells were treated as a separate compartment available for exchange of water and solutes with plasma. Ordinary differential equations describing conservation of conservation of plasma and RBC volume as well as mass flow rate of solutes were derived, coded and numerically integrated. Since experimental values were lacking for several parameters, including vasa recta permeabilities to water and sodium as well as the reflection coefficient of DVR to sodium, these were determined by iterative adjustment until solute concentrations and flow rates predicted by the model matched measured values. Although Pallone *et al.* (60) predicted substantial net removal of water and sodium from the inner medullary interstitium by the microcirculation but little removal of urea, they reported that those results were very sensitive to their assumptions about interstitial concentrations. Furthermore, outer medullary vascular bundles were ignored.

Their model was later extended by McNeely (62) to account for the fact that vasa recta terminate at various depths in the medulla. Conservation equations were modified to incorporate all vessels, and cortico-medullary gradients of urea and NaCl were assumed to increase exponentially in the inner medulla, consistent with the findings of Koepsell *et al.* (63). The multi-vessel model of McNeely (1985) yielded values of the DVR permeability to sodium that were an order-of-magnitude smaller than those estimated by Pallone *et al.* (60) and much closer to the experimental values that were later determined (see above).

Recent experimental determinations of macromolecular permeabilities, reflection coefficients, and hydraulic conductivities of vasa recta have provided indispensable data which can now permit more realistic models of the medullary microcirculation to be created. Edwards and Pallone (64-66) incorporated these data as well as the contribution of water channels and urea transporters in first a single-unit and then a multi-vessel model of the medullary microcirculation. The hypothesis that small solute trans-capillary gradients mediate transport across paracellular pathways was refuted by Turner and Pallone (49), and the reflection coefficients to sodium and urea in the paracellular transmural volume flux were taken be zero. However, since sodium and urea are excluded from water channels, the reflection coefficient of this pathway to small solutes is unity. The paracellular (J_v^P) and the transcellular (J_{vt}^P) volume fluxes in DVR are therefore given by:

Equations 7a, 7b

$$J_V^P = L_P[\Delta P - s_P \Delta p]$$
$$J_{Vt}^P = L_{Pt}[\Delta P - \Delta p - RT \sum_S g_S (C_S - C_S^I)]$$

where L_{pt} is the hydraulic permeability of the water channels. Hydraulic and oncotic pressure differences are on the order of 10 mmHg; since RT is 19.3 mmHg.mM^{-1} at 37^{o}C, and sodium and urea concentrations are on the order of 100 mM, the third term in equation 7b is dominant when the small solute interstitial-to-DVR concentration gradients are large. As illustrated below, the model of Edwards and Pallone (64-66) predicted that although the balance between hydraulic and oncotic pressure gradients favors water influx into DVR, small solute concentration gradients are significant enough to induce volume efflux from DVR in parts of the medulla. Based upon representative values of morphological and hemodynamic parameters, variations in total and single vessel plasma flow rates along the cortico-medullary axis are shown in Figures 3a and 3b, respectively. The total plasma flow rate, Q_P, decreases near the cortico-medullary junction, where the interstitial-to-DVR concentration gradients of sodium and urea are large (see below); although some water enters DVR through the paracellular pathway, a greater amount is drawn out through the water channels. As small solute concentration gradients become smaller, the balance is reversed and the paracellular volume flux becomes dominant, favoring volume influx into DVR throughout the rest of the medulla (Figure 3b). The total plasma flow rate in the inner medulla decreases nevertheless only because the number of DVR

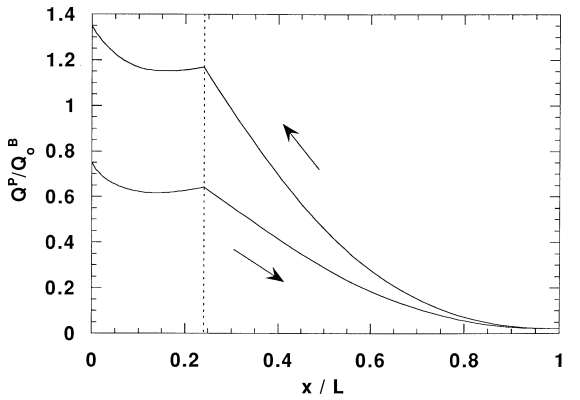

Figure 3a. Total vasa recta blood flow rates predicted by modeling. Ratio of total plasma flow (Q^P) to initial descending vasa recta (DVR) blood flow rate (Q_o^B) as a function of position in DVR and AVR; x/L denotes the ratio of axial coordinate to total length of medulla, and the vertical dashed line marks the boundary between the outer and the inner medulla. The initial value of hematocrit in DVR was taken as 0.25.

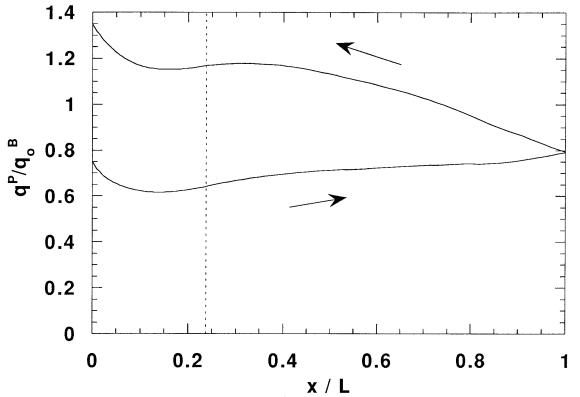

Figure 3b. Single vessel vasa recta blood flow rates predicted by modeling. Ratio of single vessel plasma flow rate (q^P) to initial single DVR blood flow rate (q_o^B) as a function of position in DVR and AVR.

drops sharply as they convert back into AVR (Figure 3a). In AVR, which are devoid of AQP1, the plasma flow rate increases all the way from the papillary tip to the cortico-medullary junction both because the number of vessels increases and because large intra-capillary protein concentrations favor volume influx in each one of them (Figure 3b).

Representative variations of sodium and urea concentration along the cortico-medullary axis are shown in Figures 4a and 4b, respectively. Given the counter-current arrangement of vasa recta, concentrations increase more slowly in DVR plasma than in the interstitium; as plasma flows back up AVR, the decrease in plasma concentrations is also parallel to that in the interstitium, but slower. Due to the presence of water channels, the permeability of DVR to urea is much greater than that of AVR, so that interstitium-to-DVR urea concentration gradients are significantly smaller than AVR-to-interstitium urea concentration differences, as illustrated in Figure 4b. In addition, since the initial urea concentration in DVR is about 30 times less that of sodium (5 vs. 150 mM), whereas the two solutes contribute almost equally to the osmolality at the papillary tip, the total concentration increase is much greater for urea than for sodium. As noted above, interstitial-to-DVR concentration gradients are initially large near the cortico-medullary junction and then rapidly dissipated, a consequence of the presence of water channels in DVR; the sieving of small solutes by AQP1 near the junction raises their concentrations rapidly.

The assumption that concentration polarization at the walls of AVR during volume uptake eliminates transmural oncotic pressure gradients was also examined (65). The difference between the hydraulic pressure in the interstitium and that in the AVR lumen needed to drive AVR volume uptake was found to be smaller than the maximum pressure difference that AVR can sustain, as measured by MacPhee and Michel (67). Edwards and Pallone (66) recently extended their model to include reabsorption rates of water and small solutes from the loop of Henle and the collecting duct into vasa recta, rather than specifying interstitial concentration profiles.

An alternative approach was proposed by Wang and coworkers (68). The basis for their model was a counter-current capillary loop surrounded by a secretory epithelium, with a specified constant solute input rate from an external source into the interstitial fluid. Assuming that blood flows at a given average velocity, Wang *et al.* (68) were able to derive analytical solutions for solute concentrations. In a subsequent refinement (69), anastomoses between DVR and AVR were modeled as a linear decrease in cross-sectional area of the vessels and in flow velocity from the base to the tip of the capillary loop. Their theoretical approach was constrained by the desire to achieve an analytical result that avoids numerical integration. Consequently, the coupling that exists between the transport of water and that of small solutes and proteins had to be ignored. Their efforts nonetheless led to important insights and showed that certain parameter combinations yielded sodium concentration profiles that were in good agreement with the experimental data of Koepsell *et al.* (63).

8. REGULATION OF MEDULLARY BLOOD FLOW

8.1. Autoregulation

Autoregulatory mechanisms enable total renal blood flow to remain constant despite changes in arterial perfusion pressure. Perfusion of the renal cortex is autoregulated, however, the autoregulation of the smaller fraction of renal blood flow that reaches the medulla is uncertain. Early experiments using dye transit times favored lack of medullary autoregulation but many subsequent studies favor its presence (70-76). Recent studies in the rat suggest that the efficiency of medullary autoregulation depends upon extracellular fluid volume status. Examinations of regional blood flow to the cortex and medulla using videomicroscopy and laser-Doppler probes placed on the renal surface (74) or implanted into the renal parenchyma at various depths (75) showed that

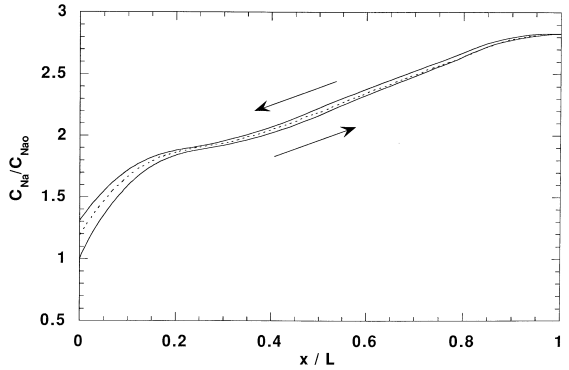

Figure 4a. Sodium concentration in plasma and interstitium predicted by modeling. Ratio of sodium concentration (C_{Na}) to its initial DVR concentration (C_{Nao}) as a function of position in DVR, AVR, and interstitium (dotted curve).

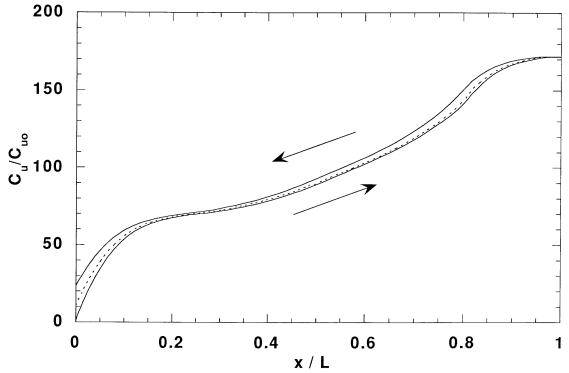

Figure 4b. Urea concentration in plasma and interstitium predicted by modeling. Ratio of urea concentration (C_U) to its initial DVR concentration (C_{UO}) as a function of position in DVR, AVR, and interstitium (dotted curve).

medullary blood flow of volume expanded rats increased with perfusion pressure due to a combined effect of increasing single vessel blood flow and recruitment of flow through previously unperfused vasa recta (Figure 3). Hydropenic rats exhibited intact medullary autoregulation. Laser-Doppler studies of regional blood flow in dogs by Majid and colleagues have tended to support intact medullary autoregulation (76).

8.2. Nitric Oxide

Endothelial cells can inhibit contraction of smooth muscle by secreting paracrine mediators including nitric oxide (NO), prostaglandin I_2 (PGI_2, prostacyclin) and endothelial hyperpolarizing factor (EDHF) (77,78). Experiments by various investigators have shown that regional perfusion of the medulla is strongly dependent upon NO. The effect of NO synthase inhibition on renal resistance vessels has been examined using the juxtamedullary nephron preparation and split hydronephrotic kidney. Imig and Roman found a selective effect to constrict interlobular arteries and afferent arterioles. These studies concluded that NO interferes with juxtamedullary autoregulation (79,80). Larson and Lockhart found that the failure of vasa recta blood flow to autoregulate in control rats could not be reproduced in spontaneously hypertensive rats (SHR). Infusion of L-arginine blunted medullary autoregulation in the SHR and normalized pressure natriuresis (81). In separate studies it was shown that infusion of a NO synthase inhibitor into rats enhances medullary autoregulation and blunts pressure natriuresis (82). Chronic infusion of a NO synthase inhibitor into conscious rats induces sustained hypertension, reduced medullary perfusion and reduced sodium excretion (83).

8.3. Vasopressin

Diuresis might be augmented by increasing medullary blood flow and reducing the efficiency of countercurrent exchange. Consistent with this notion, vasopressin probably modulates renal medullary perfusion. Homozygous Brattleboro rats lack vasopressin, have central diabetes insipidus and higher papillary plasma flows than antidiuretic Wistar or heterozygous Brattleboro rats (84). The effect of vasopressin and specific V_1 (vasoconstrictor) and V_2 (antidiuretic) receptor subtype inhibitors on vasa recta blood flow has been studied with papillary videomicroscopy. Those studies showed that vasopressin reduces single vessel blood flow rates in DVR and AVR. This effect can be partially blocked by either V_1 or V_2 inhibitors (85-88).

Blood flow to the renal medulla is largely derived from the efferent flow of juxtamedullary glomeruli. Thus, based on anatomical considerations, one can hypothesize that vasopressin reduces medullary perfusion by constricting juxtamedullary arterioles or outer medullary DVR. Consistent with this, it has been observed that vasopressin constricts juxtamedullary afferent (10^{-12} - 10^{-9} M) and efferent (10^{-9} M) arterioles in isolated, blood perfused rat kidneys (89) as well as rabbit cortical efferent arterioles (10^{-13} - 10^{-7} M) and rat outer medullary DVR (10^{-10} to 10^{-6} M) perfused *in vitro* (5,90). The low sensitivities of these vessels to vasopressin may be artifacts of preparation. V_1 receptors appear to mediate renal vasoconstriction by vasopressin, whereas V_2 receptors mediate vasodilation (88,91-94), perhaps via NO (93). It has been shown that selective activation of V_2 receptors dilates pre-constricted afferent arterioles (94) or outer medullary DVR (5) *in vitro*. Recent efforts to detect expression with the polymerase chain reaction failed to identify V_2 receptor mRNA in isolated micro-vessels (95).

Intrarenal infusion of vasopressin or a selective V_1 receptor agonist reduces inner medullary blood flow to a greater extent than outer medullary blood flow without influencing perfusion of the cortex (96). More recent studies, performed with chronically implanted laser-Doppler probes showed that physiological concentrations of circulating vasopressin selectively reduces blood flow to the inner medulla. Cortical and outer medullary blood flow did not change when rats were deprived of water. In contrast, inner medullary perfusion decreased inversely with the degree of antidiuresis. Intramedullary infusion of a V_1 antagonist blocked the decline in inner medullary blood flow and interfered with urinary concentration (97). Furthermore, when vasopressin was infused into decerebrate rats to keep plasma levels within a

physiological range of 2.9 to 11.2 pg/ml (about 10^{-12} to 10^{-11} M), inner medullary blood flow fell to an extent that again, correlated with urinary osmolality (98). This recent evidence provides the most striking evidence that vasopressin enhances urinary concentration both by the V_2 mediated increase in osmotic water permeability of the collecting duct and by V_1 mediated reduction of medullary blood flow. The latter is expected to enhance efficiency of countercurrent exchange and appears to be most pronounced in the inner medulla.

8.4. Abrogation of medullary hypoxia.

Oxygen tensions fall from cortex to the papillary tip (99). At least two mechanisms have been identified that might serve to limit medullary hypoxia. Low O_2 tensions favor release of adenosine. Hypoxia also may inhibit production of the vasoconstrictor, 20-HETE. Each of these vasodilatory influences is a direct consequence of reduction of local O_2 concentrations.

In most microvascular beds, adenosine is produced during periods of increased oxygen demand or decreased supply, leading to local vasodilation, mediated through A_2 receptor activation. In contrast, in the kidney, infused adenosine reduces cortical and net renal blood flow through A_1 receptor mediated constriction of afferent arterioles. Within the renal medulla, however, adenosine increases perfusion by acting on the A_2 receptors of pre- and postglomerular vessels (6,100,101). Adenosine decreases sodium delivery by reducing glomerular filtration rate and inhibits sodium reabsorption in the medullary thick ascending limb (MTAL). These effects could abrogate tissue hypoxia by reducing MTAL O_2 consumption (102). The MTAL generates adenosine in response to hypoxia so that proximity of the site of adenosine production to outer medullary DVR on the vascular bundle periphery might provide a mechanism by which the MTAL enhances its own perfusion and oxygenation.

Adenosine A_1 and A_2 receptor subtype mRNA expression has been demonstrated in micro-dissected OMDVR by RT-PCR. A_1 receptor mediated constriction and A_2 receptor mediated vasodilation can be readily demonstrated in the same vessels (5,103). The differing affinities of the A_1 receptor (nanomolar) and A_2 receptor (micromolar) suggest that increases in local tissue adenosine concentration might convert adjacent micro-vessels from vasoconstriction to vasodilation. Consistent with this idea, renal interstitial adenosine concentration has been measured by microdialysis at 0.2 μM, so that small increases in adenosine secretion might lead to A_2 receptor activation (104). Dinour *et al.* have shown that medullary oxygen tensions increase following interstitial adenosine infusion (99). A_1 receptor stimulation with selective agonist decreases both cortical and medullary blood flow while adenosine infusion (A_1 and A_2 activation) enhances medullary perfusion (101,105).

Vasoactive products of arachidonic acid are generated by cytochrome P-450 enzymes, epoxyeicosatrienoic acids (EETs), vic-dihydroxyeicosatetraneoic acids (DHETs) and the hydroxyeicosatetraenoic acids (HETEs) (106). The 20 omega-hydroxylation product, 20-HETE, is a potent vasoconstrictor synthesized by renal micro-vessels. Production of 20-HETE is substrate limited by local O_2 tension (107,108). Blockade of 20-HETE production blunts autoregulation and inhibition of outer medullary 20-HETE production in Lewis rats produces salt sensitive hypertension. A role for 20-HETE to modulate local blood flow in response to tissue oxygenation has been postulated (109). It has recently been shown that nitric oxide blocks vasoconstriction, at least in part, through inhibition of P-450, the enzyme responsible for generation of 20-HETE (110,111).

8.5. Angiotensin

Most studies favor tonic constriction of the juxtamedullary microcirculation by angiotensin II (ANGII). Renal arterial infusion of ANGII in dogs decreased papillary plasma flow as measured by albumin accumulation (112). Administration of either saralasin or captopril increased papillary red blood cell velocity, an effect interpreted as showing a tonic effect of ANGII to reduce perfusion (113). Similar results were obtained using laser-Doppler flowmetry (27). Direct examination of the influence of ANGII on resistance vessels using the perfused juxtamedullary nephron preparation (114), or the split hydronephrotic kidney (115) demonstrated that afferent and efferent arterioles are both constricted by ANGII in a manner that is modulated by endogenous products of cyclooxygenase (116). *In vitro* perfused DVR from vascular bundles also constrict in response to ANGII, an effect that is abrogated by either PGE_2 (2) or adenosine (6).

8.6. Prostaglandins

The renal medulla contains high levels of eicosanoids, especially PGE_2. Stimulation of prostaglandin synthesis leads to redistribution of blood flow to the juxtamedullary cortex and inhibition of perfusion of the superficial cortex (117,118). Videomicroscopic studies found a consistent decrease in papillary vasa recta blood flow after treatment with indomethacin or meclofenamate (119). Papillary videomicroscopy has also been used to examine the interaction of prostaglandins and ANGII in the renal medulla. Cyclooxygenase inhibition with indomethacin caused vasa recta blood flow to decrease, an effect that was potentiated when ANGII synthesis was blocked with captopril (113).

The general effect of inhibiting prostaglandin synthesis on regional tissue blood flow has been examined with regard to its role in physiological and pathophysiological conditions. Laser-Doppler studies of regional blood flow within the kidney showed that cyclooxygenase inhibition blunts the pressure natriuretic response and selectively reduces perfusion of the medulla without altering cortical blood flow (120). Pareck and Zou implanted platinum needle electrodes to detect locally generated H_2 as a measure of cortical and medullary blood flow in rats. In that preparation, ANGII and norepinephrine reduced medullary blood flow only after indomethacin pretreatment (121). Heyman and colleagues showed that administration of radiocontrast agents produces a decline in both cortical and medullary oxygen

content leading to hypoxic insult particularly manifest in the outer medullary thick ascending limbs of Henle (MTAL) (122). Iothalamate alone dilated the renal vasculature, however, upon pretreatment with indomethacin, iothalamate induced vasoconstriction (96). Similarly, during ureteral obstruction, indomethacin exacerbated damage to thick ascending limbs and altered cortical and medullary perfusion (123).

The capability of prostaglandins to modulate vasoconstriction of various renal resistance vessels has been repeatedly demonstrated. Edwards found that PGE_2 dilated *in vitro* perfused preglomerular resistance vessels from the rat (125). In contrast, Inscho *et al* found that PGE_2 enhanced ANGII induced vasoconstriction of glomerular resistance vessels in the juxtamedullary nephron preparation (126). Arima *et al* examined the effect of indomethacin on the reactivity of microperfused rabbit efferent arterioles to ANGII and norepinephrine. During orthograde perfusion through the glomerulus, but not retrograde perfusion toward the glomerulus, indomethacin enhanced vasoconstriction, a finding interpreted as implying a role for glomerular prostaglandins to modulate the vasomotor tone of efferent arterioles (127). Abluminal PGE_2 abrogates vasoconstriction of outer medullary DVR (3,6).

8.7. Endothelins

The ET-1 endothelin isotype is a potent vasoconstrictor that acts upon afferent and efferent arterioles, arcuate and interlobular arteries (9,10,128,129) and DVR (3). ET receptors have been identified on collecting ducts, vascular bundles and RMIC (130). There have been few studies of the effects of endothelins on regional blood flow in the kidney. Bolus injection of ET-1 (a mixed ETA and ETB receptor agonist) was shown to selectively reduce cortical blood flow while transiently increasing medullary blood flow, effects which were inhibited by blocking ETA and ETB receptors, respectively. ETB mediated increase in medullary blood flow was eliminated by blocking NO synthase or cyclooxygenase with high dose indomethacin (131). ET's might play a significant role in pathological states (132). Renal hypoxia stimulates ET production (133) and ET receptor antagonists have been shown to attenuate injury due to ischemia (134,135) or hyperfiltration in remnant kidneys created by surgical ablation (136).

8.8. Atrial Natriuretic Peptide

Many investigators have tested the hypothesis that ANP induces natriuresis and diuresis, at least in part, by increasing medullary perfusion. Studies showed that ANP infusions increased renal blood flow, glomerular filtration rate, papillary plasma flow and sodium excretion but that the diuresis and natriuresis began before the increase in medullary blood flow. Thus, it appears that an increase in medullary blood flow is not required for ANP to induce natriuresis (137,138). An effect of ANP to increase medullary blood flow was also observed using thermal diffusion (139) or isotopic renography (140).

ANP appears to vasodilate juxtamedullary resistance vessels. Aalkjaer *et al.* showed that ANP dilates renal arcuate arteries and small arteries from other micro-vessel beds (141). Marin-Grez and colleagues found dilation of arcuate, interlobular and afferent arterioles and vasoconstriction of efferent arterioles in the split hydronephrotic kidney (142). In a later study with this preparation, Hayashi and colleagues found reversal of norepinephrine induced afferent arteriolar vasoconstriction but no effect on perfusion pressure induced vasoconstriction (143). In the juxtamedullary nephron preparation, superfusion with atriopeptin III caused arcuate and afferent arterioles to dilate 73 and 23%, respectively, while efferent arteriolar diameters did not change (144). Edwards and Weidley found no effect of ANP on *in vitro* perfused rabbit afferent or efferent arterioles (145).

9. PERSPECTIVES

The organization of the renal microcirculation suggests that the goal of vasomotion is to modulate regional perfusion. Within the cortex, constriction of interlobular arteries or intra-arterial cushions might distribute blood flow toward the medulla. Increase in resistance of juxtamedullary arterioles relative to their superficial counterparts should favor perfusion of the superficial cortex. DVR are the final contractile elements in the renal medullary blood flow circuit. It seems unlikely that DVR impart a large fraction of the overall resistance to medullar blood flow. It is more likely that they modulate the fraction of total medullary blood flow that is distributed to the inner versus outer medulla. Increasingly convincing evidence has been provided to favor a role for control of medullary perfusion as a component of the processes which regulate sodium excretion and urinary concentration. Vascular tone within the kidney is subject to myriad hormonal, paracrine, autocrine and neural controls. Efforts to elucidate the signaling mechanisms that control vasomotor tone as well as the transport pathways that govern countercurrent exchange are pertinent to our understanding of these processes. It is often difficult, however, to extrapolate the results to achieve a full understanding of the complex interplay of factors that determine local tissue perfusion and efficient countercurrent exchanger function.

11. ACKNOWLEDGEMENTS

The authors where supported by NIH grants: DK53775 (AE), HL57329 (EPS) DK42495 and HL62220 (TLP).

12. REFERENCES

1. Holliger, C., Lemley, K.V., Schmitt, S.L., Thomas, F.C., Robertson, C.R. & R.L. Jamison: Direct determination of vasa recta blood flow in the rat renal papilla. *Circ. Res.* 53: 401-413 (1983)

2. Pallone, T.L.: Vasoconstriction of outer medullary vasa recta by angiotensin II is modulated by prostaglandin E_2. *Am. J. Physiol.* 266: F850-F857 (1994)

3. Silldorff, E.P., Yang, S. & T.L. Pallone: Prostaglandin E_2 abrogates endothelin-induced vasoconstriction in renal

outer medullary descending vasa recta of the rat. *J. Clin. Invest.*, 95: 2734-2740 (1995)
4. Yang, S., Silldorff, E.P. & T.L. Pallone: Effect of norepinephrine and acetylcholine on outer medullary descending vasa recta. *Am. J. Physiol.* 269: H710-H716 (1995)
5. Turner, M.R. & T.L. Pallone: Vasopressin constricts outer medullary descending vasa recta isolated from rat kidneys. Am. J. Physiol., 272:F147-F151 (1997)
6. Silldorff E.P., Kreisberg, M.A. & T.L. Pallone: Adenosine modulates vasomotor tone in outer medullary descending vasa recta. *J. Clin. Invest.*, 98: 12-23 (1996)
7. Pallone, T.L., Robertson, C.R. & R.L. Jamison: Renal Medullary Microcirculation. *Physiol. Reviews*, 70:885-920 (1990)
8. Jamison, R.L. & W. Kriz. *Urinary Concentration Mechanism: Structure and Function.* Oxford Univ. Press, New York, (1982)
9. Navar, L.G., Inscho, E.W., Majid, S.A., Imig, J.D., Harrison-Bernard, L.M. & K.D. Mitchell: Paracrine regulation of the renal microcirculation. *Physiol. Rev.*, 76: 425-536 (1996).
10. Pallone, T.L., Silldorff, E.P. & M.R. Turner: Intrarenal blood flow: Microvascular anatomy and regulation. *Clin Exp. Pharm. Physiol.* 25:383-392 (1998).
11. Velasquez, M.T., Notargiocomo, A.B., & J.N. Cohn: Influence of cortical plasma transit time on p-amino-hippurate extraction during induced renal vasodilation in anaesthetized dogs. *Clin. Sci. Lond.* 43: 401-411 (1972)
12. Grantham, J.J., Qualizza, P.B., & R.L. Irwin: Net fluid secretion in proximal straight renal tubules *in vitro*: role of PAH. *Am. J. Physiol.* 226: 191-197 (1974)
13. Thornburn, G.D., Kopald, H.H., Herd, J.A., Hollenberg, M., O'Morchoe, C.C.C., & C. Barger: Intrarenal distribution of nutrient blood flow determined with krypton^{85} in the unanesthetized dog. *Circ. Res.* 13: 290-307 (1963)
14. Aukland, K., & R.W. Berliner: Renal medullary countercurrent system studies with hydrogen gas. *Circ. Res.* 15: 431-442 (1964).
15. Aukland, K., Bower, B.F. & R.W. Berliner: Measurement of local blood flow with hydrogen gas. *Circ. Res.* 14: 164-187 (1964)
16. Aukland, K.: Vasopressin and intrarenal blood flow distribution. *Acta Physiol. Scand.* 74: 173-182 (1968)
17. Parekh, N., Sadowski, J. & M. Steinhausen: Tissue PH_2 measurements for continuous estimation of blood flow changes in rat kidney cortex and medulla. *Pfluegers Arch.* 419: 450-453 (1991)
18. Sapirstein, L.A.: Regional blood flow by fraction distribution of indicators. *Am. J. Physiol.* 193: 161-168, (1958)
19. Karlberg, L., Kallskog, O., Ojteg, G. & M. Wolgast: Renal medullary blood flow studied with the 86-Rb extraction method. Methodological consideration. *Acta Physiol. Scand.* 115: 11-18 (1982)
20. Goldberg, A.H. & L.S. Lilienfield: Effect of hypertonic manntiol on accumulation rate and distribution of albumin in the renal papilla. *Proc. Soc. Exp. Biol. Med.* 113: 795-798 (1963)
21. Lilienfield, L.S., Maganzini, H.C. & M.H. Bauer. Blood flow in the renal medulla *Circ. Res.* 9: 614-617 (1961)
22. Slotkoff, L.M. & L. S. Lilienfield: Extravscular renal albumin. *Am. J. Physiol.* 212: 400-406 (1967)
23. Rasmussen, S.N.: Intrarenal red cell and plasma volumes in the non-diuretic rat. *Pfluegers Arch.* 342: 61-72 (1973)
24. Rasmussen, S.N.: Step function input to the rat kidney by shifting between auto- and alloperfusion. *Am. J. Physiol.* 233: H488-H492 (1977)
25. McNay, J.L. & Y. Abe. Pressure dependent heterogeneity of renal cortical blood flow in dogs. *Circ. Res.* 27: 571-587 (1970)
26. Bankir, L., Farman, N., Gungeld, J.-P., Huet de la Tour, E. & J.-L. Funck-Bretano: Radioactive microsphere distribution and single glomerular blood flow in the normal rabbit kidney. *Pfluegers Arch.* 342: 111-123 (1973)
27. Roman, R.J. & C. Smits: Laser-Doppler determination of papillary blood flow in young and adult rats. *Am. J. Physiol.* 251 F115-F124 (1986)
F28. enoy, F.J. & R.J. Roman: Effect of volume expansion on papillary bloood flow and sodium excretion. *Am. J. Physiol.* 260:F813-F822 (1991)
29. Marsh, D.J. & L.A. Segel: Analysis of counter-current diffusion exchange in blood vessels of the renal medulla. *Am. J. Physiol.*, 221: 817-828 (1971)
30. Gussis, G.L., Jamison, R.L. & C.R. Robertson: Determination of erythrocyte velocities in the mammalian inner real medulla by a video velocity-tracking system. *Microvasc. Res.* 18: 370-383 (1979)
31. Zimmerhackl, B., Dussel, R. & M. Steinhausen: Erythrocyte flow and dynamic hematocrit in the renal papilla of the rat. *Am. J. Physiol.* 249: F898-F902 (1985)
32. Zimmerhackl, B., Tinsman, J., Jamison, R.L. & C.R. Robertson: Use of digital cross-correlation for on line determination of single vessel blood flow in the mammalian kidney. *Microvasc. Res.* 30: 63-74 (1985)
33. Chaung, E.L., Reineck, H.J., Osgood, R.W., Kunau, R.T., & J.H. Stein: Studies on the mechanism of reduced urinary osmolality after exposure of the real papilla. *J. Clin. Invest.* 61: 633-639 (1978)
34. Pappenheimer, J.R. & W.B. Kinter: Hematocrit ratio of blood within mammalian kidney and its significance for renal hemodynamics. *Am. J. Physiol.*, 185: 377-390 (1956)
35. Fahraeus, R.: The suspension stability of blood. *Physiol. Rev.* 9: 241-274 (1929)
36. Gaehtgens, P.: Flow of blood through narrow capillaries: rheological mechanisms determining capillary hematocrit and apparent viscosity. *Biorheology* 17: 183-189 (1980)
37. Pries, A.R., Ley, K. & P. Gaehtgens: Generalization of the Fahraeus principle for micro-vessel networks. *Am. J. Physiol.* 251 : H1324-H1332 (1986)
38. Pallone, T.L., Work, J. & R.L. Jamison: Resistance of descending vasa recta to the transport of water. *Am. J. Physiol.* 259 : F688-F697 (1990)
39. Pallone, T.L.: Resistance of ascending vasa recta to water transport. *Am. J. Physiol.* 260: F303-F310 (1991)
40. Schwartz, M.M., Karnovsky, M.J., & M.A. Venkatachalam: Ultrastructural differences between rat inner medullary descending and ascending vasa recta. Lab. Invest. 35:161-170 (1976)
41. MacPhee, P.J. & C.C. Michel: Fluid uptake from the renal medulla into the ascending vasa recta in anaesthetized rats. *J. Physiol.*, 487: 169-183 (1995)

42. Pallone, T.L., Kishore, B.K., Turner, M.R., Nielsen, S., Agre, P. & M.A. Knepper: Evidence that Aquaporin I mediates NaCl water flux across rat descending vasa recta. *Am. J. Physiol.* 272: F587-F596 (1997).
43. Morgan, T. & R. W. Berliner: Permeability of the loop of Henle, vasa recta, and collecting duct to water, sodium and urea. Am. J. Physiol. 215: 108-115 (1968)
44. Pallone, T.L., Work, J., Myers, R.L. & R.L. Jamison: Transport of sodium and urea in outer medullary descending vasa recta. *J. Clin. Invest.*, 93:212-222 (1994)
45. Pallone, T.L.: Characterization of the urea transporter in outer medullary descending vasa recta. *Am. J. Physiology*. 267: R260-R267 (1994)
46. Tsukaguchi, H., Shayakul, C., Berger, U.V. Tokui, T., Brown, D. & M. Hediger: Cloning and characterization of the urea transporter UT3. *J. Clin. Invest.*, 99: 1506-1515 (1997)
47. Xu, Y., Olives, B., Bailly, P., Fisher, E., Ripoche, P., Ronco, P., Cartron, J.-P. & E. Rondeau. Endothelial cells of the kidney vasa recta express the urea transporter HUT11. *Kidney Int.*, 51: 138-146 (1997)
48. Pallone, T.L.: Molecular sieving of albumin by the ascending vasa recta wall. *J. Clin. Invest.*, 90:30-34 (1992)
49. Turner, M.R. & T.L. Pallone: Hydraulic and diffusional permeabilities of isolated outer medullary descending vasa recta from the rate. *Am. J. Physiol.* 272: H392-H400, (1997)
50. Lilienfield, L.S. & J.C. Rose: Effect of blood pressure alterations on intrarenal red cell plasma separation. *J. Clin. Invest.* 37:1106-1110 (1958)
51. Pallone T.L.: Extravascular protein in the renal medulla: Analysis by two methods. *Am. J. Physiol.* 266: R1429-R1436 (1994)
52. Michel, C.C.: Fluid movements through capillary walls. In: *Handbook of Physiology*, sect. 2, *The Cardiovascular System*, vol. IV, *The Microcirculation*, ed. Renkin, E.M., and C.C. Michel, pp 375-409, Am. Physiol. Soc., Washington, DC, (1984)
53. Levick, J.R.: Capillary filtration - Absorption balance reconsidered in light of dynamic extravascular factors. *Exp. Physiol.*, 76: 825-857 (1991)
54. Nielsen, S., Pallone, T. L., Smith, B.L., Christensen, E.I., Agre, P. & Q.B. Maunsbach: Aquaporin-1 water channels in short and long loop descending thin limbs and in descending vasa recta in rat kidney. *Am. J. Physiol.* 268: F1023-F1037 (1995)
55. Pallone, T.L. & M.R. Turner: Molecular sieving of small solutes by outer medullary descending vasa recta. *Am. J. Physiol.* 272: F579-F586 (1997)
56. Stephenson, J.L.: Concentration of the urine in a central core model of the counterflow system. *Kidney Int.*, 2: 85-94 (1972)
57. Layton, H.E. & J.M. Davies: Distributed solute and water reabsorption in a central core model of the renal medulla. *Math. Biosciences*, 116: 169-196 (1993)
58. Thurau, K., Deetjen, P. & H. Günzler. Die diurese bei arteriellen drucksteigerungen. *Pfluegers Arch.*, 274: 567-580 (1962)
59. Palatt, P.J. & G.M. Saidel. An analysis of counter-current exchange with emphasis on renal function. *Bull. Math. Biol.* 35: 275-286 (1973)
60. Pallone, T.L., Morgenthaler, T.I. & W.M. Deen: Analysis of microvascular water and solute exchanges in the renal medulla. *Am. J. Physiol.* 247: F303-F315 (1984)
61. Kedem, O. & A. Katchalsky: Thermodynamic analysis of the permeability of biological membranes to nonelectrolytes. *Biochem. Biophys. Acta*. 27: 229-246 (1958)
62. McNeely, E.A., Pallone, T.L., Deen, W.M. & C.R. Robertson: Models of the medullary microcirculation. *Kidney Int.* 31:662-667 (1987)
63. Koepsell, H., Nicholson, W.E.A.P., Kriz, W. & H.J. Höhling: Measurements of exponential gradients of sodium and chlorine in rat kidney medulla using the electron microprobe. Pflügers Arch., 350: 167-184 (1974)
64. Edwards, A. & T.L. Pallone: Facilitated transport in vasa recta: theoretical effects on solute exchange in the medullary microcirculation. *Am. J. Physiol.* 272: F505-F514, (1997)
65. Edwards, A. & T.L. Pallone: A multi-unit model of solute and water removal by inner medullary vasa recta. *Am. J. Physiol.* 274: H1202-H1210 (1998).
66. Edwards, A.E., DeLong, M.J. & T.L. Pallone: Interstitial water and solute recovery by inner medullary vasa recta. *Am. J. Physiol.* 278: F257-F269 (2000)
67. MacPhee, P.J. & C.C. Michel: Subatmospheric closing pressures in individual micro-vessels of rats and frogs. *J. Physiol.* 484: 183-187 (1995)
68. Wang, W., K.H. Parker, and C.C. Michel. Theoretical studies of steady-state trans-capillary exchange in countercurrent systems. *Microcirc.*, 3: 301-311, 1996.
69. Wang, W. & C.C. Michel: Effects of anastomoses on solute trans-capillary exchange in countercurrent systems. *Microcirc.*, 4:381-390 (1997)
70. Thurau, K.: Renal hemodynamics. *Am. J. Med*. 36:698-719 (1964)
71. Galskov A. & O.I. Nissen: Autoregulation of directly measured blood flows in the superficial and deep venous drainage areas of the cat kidney. *Circ. Res*. 30:97-103 (1972)
72. Stern, M.D., Bowen, P.D., Parma, R., Osgood, R.W., Bowman, R.L. & J.H. Stein: Measurement of renal cortical and medullary blood flow by laser-Doppler spectroscopy in the rat. *Am. J. Physiol*. 236:F80-F87 (1979)
73. Cohen, H.J., Marsh, D.J. & B. Kayser: Autoregulation in vasa recta of the rat kidney. *Am. J. Physiol*. 245:F32-F40, (1983)
74. Roman, R.J., Cowley, A.W., Garcia-Estan, J. & J.H. Lombard: Pressure-diuresis in volume expanded rats: Cortical and medullary hemodynamics. *Hypertension* 12:168-176 (1988)
75. Mattson, D.L., Lu, S., Roman, R.J. & A.W. Cowley: Relationship between renal perfusion pressure and blood flow in different regions of the kidney. *Am J. Physiol*. 264:R578-R583 (1993)
76. Majid, D.S.a., Godfrey, M. & S.A. Omoro: Pressure natriuresis and autoregulation of inner medullary blood flow in canine kidney. *Hypertension* 29:210-215 (1997)
77. Curry, F.E.: Modulation of venular micro-vessel permeability by calcium influx into endothelial cells. *FASEB J* 6:2456-2466 (1992)
78. Adams, D.J.: Ionic channels in vascular endothelial cells. Trends. Card. Med. 1994; 4:18-26 (1994)
79. Imig, J.D. & R.J. Roman: Nitric oxide modulates vascular tone in preglomerular arterioles. *Hypertension*. 19:770-774 (1992)

80. Hoffend, J,. Cavarape, A., Endlich, K. & M. Steinhausen: Influence of endothelium-derived relaxing factor on renal microvessels and pressure-dependent vasodilation. *Am. J. Physiol*. 265:F285-F292 (1993)
81. Larson, T.S. & J.C. Lockhart: Restoration of vasa recta hemodynamics and pressure natriuresis in SHR by L-arginine. *Am. J. Physiol*. 268:F907-F912 (1995)
82. Mattson, D.L., Lu, S., Nakanishi, K., Papanek, P.E. & A.W. Cowley. Effect of chronic renal medullary nitric oxide inhibition on blood pressure. *Am. J. Physiol*. 266:H1918-H1926 (1994)
83. Nakanishi, K., Mattson, D.L. & A.W. Cowley, Jr.: Role of renal medullary blood flow in the development of L-NAME hypertension in rats. *Am. J. Physiol*. 268:R317-R323 (1995)
84. Bayle, F., Eloy, L., Trinh-Trang-Tan, M.-M., Grunfeld, J.-P. & L. Bankir: Papillary plasma flow in rats: I. Relation to urine osmolality in normal and Brattleboro rats with hereditary diabetes insipidus. *Pflugers Arch*. 394:211-216 (1982)
85. Gussis, G.L., Robertson C.R. & R.L. Jamison: Erythrocyte velocity in vasa recta: effect of antidiuretic hormone and saline loading. *Am. J. Physiol*. 237:F326-F332 (1979)
86. Kiberd, B.A., Robertson, C.R., Larson, T.S. & R.L. Jamison: Effect of V_2 receptor-mediated changes on inner medullary blood flow induced by AVP. *Am. J. Physiol*. 253:F576-F581 (1987)
87. Zimmerhackl, B., Robertson, C.R. & R.L. Jamison. Effect of arginine vasopressin on renal medullary blood flow. A videomicroscopic study in the rat. *J. Clin. Invest*. 76:770-778. (1985)
88. Naitoh, M., Suzuki, H., Murakami, M., Matsumoto, A., Ichihara, A., Nakamoto, H., Yamamura, Y. & T. Saruta: Arginine vasopressin produces renal vasodilation via V_2 receptors in conscious dogs. *Am. J. Physiol*. 265:R934-R942 (1993)
89. Harrison-Bernard, L.M., & P.K. Carmines: Juxtamedullary microvascular responses to arginine vasopressin in rat kidney. Am. J. Physiol. 267:F249-F256 (1994)
90. Edwards, R.M., Trizna, W. & L.B. Kinter. Renal microvascular effects of vasopressin and vasopressin antagonists. Am. J. Physiol. 256:F274-F278 (1989)
91. Aki, Y., Kiyomoto, H., He, H., Yoshida, H., Iwao, H. & Y. Abe: Nitric oxide may participate in V_2 vasopressin receptor mediated renal vasodilation. *J. Card. Pharm*. 23:331-336 (1994)
92. Rudichenko, V.M. & W.H. Beierwaltes: Arginine vasopressin induced renal vasodilation mediated by nitric oxide. *J. Vasc. Res*. 32:100-105 (1995)
93. Lliard, J.-F.: L-NAME antagonizes vasopressin V_2 induced vasodilation in dogs. *Am. J. Physiol*. 266:H99-H106 (1994)
94. Tamaki, T., Kiyomoto, K., He, H., Tomohiro, A., Nishiyama, A., Aki, Y., Kimura, S. & Y. Abe: Vasodilation induced by vasopressin V_2 receptor stimulation in afferent arterioles. *Kidney Int*. 49:722-729 (1996)
95. Park, F., Mattson, D.L., Skelton, M.M. & A.W. Cowley, Jr.: Localization of the vasopressin V_{1a} and V_2 receptors within the renal cortical and medullary circulation. *Am. J. Physiol*. 273:R243-251 (1997)
96. Nakanishi, K., Mattson, D.L., Gross, V., Roman, R.J. & A.W. Cowley, Jr. Control of renal medullary blood flow by vasopressin V_1 and V_2 receptors. *Am. J. Physiol*. 269: R193-R200 (1995)
97. Franchini, K.G. & A.W. Cowley: Renal cortical and medullary blood flow responses during water restriction: role of vasopressin. *Am. J. Physiol*. 270: R1257-R1264 (1996)
98. Franchini, K.G. & A.W. Cowley: Sensitivity of the renal medullary circulation to plasma vasopressin. *Am. J. Physiol*. 271:R647-R653 (1996)
99. Dinour, D. & M. Brezis: Effects of adenosine on intrarenal oxygenation. *Am. J. Physiol*. 261:F787-F791 (1991)
100. McCoy, D.E., Bhattacharya, S., Olson, B.A., Levier, D.G., Arend, L.J. & W.S. Spielman: The renal adenosine system: structure, function and regulation. *Seminars in Nephrol*. 13:31-40 (1993)
101. Miyamoto, M., Yagil, Y., Larson, T.S., Robertson, C.R. & R.L. Jamson: Effects of intrarenal adenosine on renal function and medullary blood flow in the rat. *Am. J. Physiol*. 255:F1230-F1234 (1988)
102. Beach, R.E., Watts, B.A., Good, D.W., Benedict, C.R. & T.D. DuBose: Effects of graded oxygen tension on adenosine release by renal medullary thick ascending limb suspensions. *Kidney Int*. 39:836-842 (1991)
103. Kreisberg, M.S., Silldorff, E.P. & T.L. Pallone. Localization of adenosine receptor subtype mRNA in rat outer medullary descending vasa recta by RT-PCR. *Am. J. Physiol*. 272:H1231-H1238 (1997)
104. Baranowski, R.L. & C. Westenfelder: Estimation of renal interstitial adenosine and purine metabolites by microdialysis. *Am. J. Physiol*. 267: F174-F182 (1994)
105. Agmon, Y., Dinour, D. & M. Brezis: Disparate effects of adenosine A_1 and A_2 receptor agonists on intrarenal blood flow. *Am. J. Physiol*. 265: F802-F806 (1993)
106. Harder, D.R., Campbell, W.B. & R.J. Roman: Role of cytochrome P-450 enzymes and metabolites of arachidonic acid in the control of vascular tone. *J. Vasc. Res*. 32:79-92 (1995)
107. Imig, J.D., Zou, A.-P., Stec, D.E., Harder, D.R., Falck, J.R. & R.J. Roman: Formation and actions of 20-HETE in rat renal arterioles. *Am. J. Physiol*. 270: R217-R227 (1996)
108. Harder, D.R., Narayanan, J., Birks, E.K., Laird, J.F., Imig, J.D., Lombard, J.H., Lange, A.R. & R.J. Roman: Identification of a putative microvascular oxygen sensor. *Circ. Res*. 79: 54-61 (1996)
109. Zou, A.-P., Imig, J.D., Kaldunski, M., Ortiz de Montellano, P.R., Sui, Z. & R.J. Roman: Inhibition of renal vascular 20-HETE production impairs autoregulation of renal blood flow. *Am. J. Physiol*. 266: F275-F282 (1994)
110. Alonso-Galicia, M., Drummond, H.A., Reddy, K.K., Falck, J.R. & R.J. Roman. Inhibition of 20-HETE production contributes to the vascular responses to nitric oxide. *Hypertension* 29:320-325 (1997)
111. Stec, D.E., Mattson, D.L. & R.J. Roman: Inhibition of renal outer medullary 20-HETE production produces hypertension in Lewis rats. *Hypertension* 29:315-319 (1997)
112. Faubert, P.F., Chou, S.-Y. & J.G. Porush: Regulation of papillary plasma flow by angiotensin II. *Kidney Int*. 32:472-478 (1987)
113. Cupples, W.A., Sakai, T. & D.J. Marsh: Angiotensin II and prostaglandins in control of vasa recta blood flow. *Am. J. Physiol*. 254: F417-F424 (1988)
114. Carmines, P.K., Morrison, T.K. & L.G. Navar: Angiotensin II effects on microvascular diameters of *in vitro* blood-perfused juxtamedullary nephrons. *Am. J. Physiol*. 251:F610-F618 (1986).
115. Steinhausen, M., Kucherer, H., Parekh, N., Weis, S., Wiegman, D.L. & K.R. Wilhelm: Angiotensin II control of the renal microcirculation: Effect of blockade by saralasin. *Kidney Int*. 30:56-61 (1986)

116. Harrison-Bernard LM, Carmines PK. Impact of cyclo-oxygenase blockade on juxtamedullary microvascular responses to angiotensin II in rat kidney. *Clin. Exp. Pharm. Physiol.* 22:732-738 (1995)
117. Itskovitz, H.D., Stemper, D., Pacholczyk, D. & J.C. McGiff: Renal prostaglandins: determinants of intrarenal distribution of blood flow in the dog. *Clin. Sci. Mol. Med.* 45:321s-324s (1973)
118. Larsson, C., & E. Anggard: Increased juxtamedullary blood flow on stimulation of intrarenal prostaglandin biosynthesis. *Eur. J. Pharmacol.* 25:326-334 (1974)
119. Lemley, K.V., Schmitt, J.L., Holliger, C., Dunn, M.J., Robertson, R.J. & R.L. Jamison: Prostaglandin synthesis inhibitors and vasa recta erythrocyte velocities in the rat. *Am. J. Physiol*. 1984; 247:F562-F567 (1984)
121. Roman, R.J. & E. Lianos. Influence of prostaglandins on papillary blood flow and pressure-natriuretic response. *Hypertension* 15:29-35 (1990)
Parekh, N. & A.I. Zou: Role of prostaglandins in renal medullary microcirculation: response to different vasoconstrictors. *Am. J. Physiol*. 271:F653-658 (1996)
122. Heyman, S.N., Brezis, M., Epstein, F.H., Spokes, K., Silva, P. & S. Rosen. Early renal medullary hypoxic injury from radiocontrast and indomethacin. *Kidney Int.* 40:632-642 (1991)
123. Agmon, Y., Peleg, H., Greenfeld, Z., Rosen, S. & M. Brezis: Nitric oxide and prostanoids protect the renal outer medulla from radiocontrast toxicity in the rat. *J. Clin. Invest.* 94:1069-1075 (1994)
124. Heyman, S.N., Fuchs, S., Jaffe, R., Shina, A., Ellezian, L., Brezis, M. & S. Rosen: Renal microcirculation and tissue damage during acute ureteral obstruction in the rat. *Kidney Int.* 51:653-663 (1997)
125. Edwards, R.M.: Effects of prostaglandins on vasoconstrictor action in isolated renal arterioles. *Am. J. Physiol*. 248:F779-F784 (1985)
126. Inscho, E.W., Carmines, P.K. & L.G. Navar: Prostaglandin influences on afferent arteriolar responses to vasoconstrictor agonists. *Am. J. Physiol*. 259:F157-163 (1990)
127. Arima, S., Ren, Y.L., Juncos, L.A., Carretero, O.A. & S. Ito: Glomerular prostaglandins modulate vascular reactivity of the downstream efferent arterioles. *Kidney Int*. 45:650-658 (1994)
128. Bloom, I.T.M., Bentley, F.R., Wilson, M.A. & R.N. Garrison: *In vivo* effects of endothelin on the renal microcirculation. *J. Surg. Res.* 54:274-280 (1993)
129. Cavarape, A. & E. Bartoli: Visualization of effects of ET_A receptor blockade with BQ-123 on renal hemodynamics in the split hydronephrotic kidney of rats. *J. Am. Soc. Nephrol*. 6:656 (1995)
130. Terada, Y., Tomita, K., Nonoguchi, H. & F. Marumo: Different localization of two types of endothelin receptor mRNA in microdissected rat nephron segments using reverse transcription and polymerase chain reaction assay. *J. Clin. Invest.* 90:107-112 (1992)
131. Gurbanov, K., Rubinstein, I., Hoffman, A., Abassi, Z., Better, O.S. & J. Winaver: Differential regulation of renal regional blood flow by endothelin-1. *Am. J. Physiol.* 271:F1166-F1172 (1996)
132. Kohan, D.E.: Endothelins in the normal and diseased kidney. *Am. J. Kid. Dis.* 29:2-26 (1997)
133. Nir, A., Clavell, A.L., Heublein, D., Aarhus, L.L. & J.C. Burnett, Jr.: Acute hypoxia and endogenous renal endothelin. *J. Am. Soc. Nephrol.* 4:1920-1924 (1994)
134. Chan, L., Chittinandana, A., Shapiro, J.I., Shanley, P.F. & R.W. Schrier: Effect of an endothelin-receptor antagonist on ischemic acute renal failure. *Am. J. Physiol.* 266:F135-F138 (1994)
135. Gellai, M., Jungus, M., Fletcher, T., DeWolf, R., & P. Nambi: Reversal of postischemic acute renal failure with a selective endothelin A receptor antagonist in the rat. *J. Clin. Invest.* 93:900-906 (1994)
136. Benigni, A., Zola, C., Corna, D., Orisio, S., Facchinetti, D., Benati, L. & G. Remuzzi: Blocking both type A and B endothelin receptors in the kidney attenuates renal injury and prolongs survival in rats with remnant kidney. *Am. J. Kid. Diseases* 27:416-423 (1996)
137. Kiberd, B.A., Larson, T.S., Robertson, C.R. & R.L. Jamison: Effect of atrial natriuretic peptide on vasa recta blood flow in the rat. *Am. J. Physiol.* 252:F1112-F1117 (1987)
138. Takezawa, K., Cowley, A.W., Skelton, M. & R.J. Roman: Atriopeptin III alters renal medullary hemodynamics and the pressure-diuresis response in rats. *Am. J. Physiol*. 252:F992-F1002 (1987)
139. Tsuchiya, K., Sanaka, T., Nitta, K., Ando, A. & N. Sugino: Effects of atrial natriuretic peptide on regional renal blood flow measured by a thermal diffusion technique. *Jap J. Exp. Med.* 59:27-35 (1989)
140. Janssen, W.M., Beekhuis, H., de Bruin, R., de Jong, P.E. & D. deZeeuw: Noninvasive measurement of intrarenal blood flow distribution: kinetic model of renal 123I-hippuran handling. *Am. J. Physiol.* 269:F571-F580 (1995)
141. Aalkjaer, C., Mulvany, M.J. & N.C.B. Nyborg: Atrial natriuretic factor causes specific relaxation of rat renal arcuate arterioles. *Br. J. Pharmacol.* 86:447-453 (1985)
142. Marin-Grez, M., Fleming, J.T. & M. Steinhausen. Atrial natriuretic peptide causes pre-glomerular vasodilatation and post-glomerular vasoconstriction in rat kidney. *Nature* 324:473-476 (1986)
143. Hayashi, K., Epstein, M. & R. Louzenhiser: Determinants of renal atrial natriuretic peptide. Lack of effect of atrial natriuretic peptide on pressure induced vasoconstriction. *Circ Res.* 67:1-10 (1990)
144. Veldkamp, P.J., Carmines, P.K., Inscho, E.W. & L.G. Navar: Direct evaluation of the microvascular actions of ANP in juxtamedullary nephrons. *Am. J. Physiol*. 254:F440-F444 (1988)
145. Edwards, R.M. & E.F. Weidley: Lack of effect of atriopeptin II on rabbit glomerular arterioles *in vitro*. *Am. J. Physiol*. 252:F317-F321 (1987)
146. Pallone, T.L., Nielsen, S., Silldorff, E.P. & S. Yang. Diffusive transport of solute in the rat medullary microcirculation. *Am. J. Physiol.* 269:F55-F63 (1995)

Key Words: Renal Physiology, Vasa Recta, Endothelium, Pericytes, Urinary Concentration, Blood Flow, Microcirculation, Review

Send correspondence to: Thomas L. Pallone, MD, Division of Nephrology, University of Maryland at Baltimore, 22 S. Greene St., Room N3W 143, Baltimore, MD 21201, Tel: 410-328-5720, Fax: 410-328-5685, E-mail: tpallone@medicine.umaryland.edu

This manuscript is available on line at:

http://www.bioscience.org/2000/d/edwards/fulltext.htm